Clay Minerals, (2015) **50**, 329–340

Preparation and characterization of kaolinite nanostructures: reaction pathways, morphology and structural order

BALÁZS ZSIRKA[1], ERZSÉBET HORVÁTH[1,*], ÉVA MAKÓ[2], RÓBERT KURDI[1] AND JÁNOS KRISTÓF[3]

[1] *Institute of Environmental Engineering, University of Pannonia, H-8201 Veszprém, P.O.Box 158, Hungary*
[2] *Institute of Materials Engineering, University of Pannonia, H-8201 Veszprém, P.O.Box 158, Hungary*
[3] *Department of Analytical Chemistry, University of Pannonia, H-8201 Veszprém, P.O.Box 158, Hungary*

(*Received 8 December 2014; revised 28 April 2015; Associate Editor: H. Stanjek*)

ABSTRACT: Clay-based nanostructures were prepared from kaolinites of varying structural order by two different methods. In the first method the kaolinite-urea precursor, obtained by dry grinding, was intercalated further with triethanolamine and the tetraalkylammonium salt was synthesized in the interlamellar space. Exfoliation was achieved by the use of sodium polyacrylate (PAS). In the second method, the kaolinite-potassium acetate (kaolinite-KAc) precursor, obtained via two different methods, was intercalated further with ethylene glycol (EG) and then *n*-hexylamine (HA). Intercalation with EG was also achieved by heating either directly or with microwaves. The morphology that results depends on the method of precursor preparation, the method of heat treatment and the degree of structural order of the original clay. Higher structural order facilitates the formation of a tubular morphology, while mechanical treatment and microwave agitation may result in broken tubes. Molecular mechanical (MM) calculations showed that organo-complexes may be exfoliated to a *d* value of 10–11 Å.

KEYWORDS: intercalation, kaolinite nanostructure, molecular mechanical calculation.

The applications of kaolin, a widely used industrial clay raw material, depend on its surface reactivity. The main mineral component of kaolin is kaolinite, which consists of layers held together via H-bonds. Each layer consists of a two-dimensional arrangement of Al-centred octahedra (O) and a two-dimensional arrangement of Si-centred tetrahedra (T). The theoretical formula is $Al_2Si_2O_5(OH)_4$ (Bergaya *et al.*, 2006). In addition to its common applications (e.g. filler in polymers, rubber, paper, cosmetics, medicines, etc.) kaolin can be used in composites, nano-hybrids, adsorbents (Matusik & Bajda, 2013; Dedzo & Detellier, 2014; Matusik & Matykowska, 2014), in electrode coatings (Tonlé *et al.*, 2011) and in catalysts (Nakagaki *et al.*, 2006; Bizaia *et al.*, 2008; De Faria *et al.*, 2012; Araújo *et al.*, 2014). These applications, however, require modifications of the surface and, often, their structure. One possible way of modifying the surface/structure is the preparation of kaolinite organo-complexes or kaolinite-metal complexes making them suitable for use in composites or in surface coatings (Rehim *et al.*, 2010; Matusik *et al.*, 2011; Tao *et al.*, 2014).

The surface modification of kaolins by intercalation and replacement intercalation has been studied extensively in the past. Tunney & Detellier (1994) used ethylene glycol (EG) to replace dimethyl sulfoxide (DMSO) in the kaolinite-DMSO complex. Those authors also studied the effect of water on the stability of the kaolinite-EG intercalate. Tunney & Detellier (1996) were the first to intercalate an organic polymer between the kaolinite layers, producing a kaolinite-

* E-mail: erzsebet.horvath@gmail.com
DOI: 10.1180/claymin.2015.050.3.06

PEG complex from a kaolinite-DMSO intercalate in molten polyethylene glycol (PEG 3400 and PEG 1000). Tunney (1996) connected methoxy groups to the inner surface hydroxyls by treatment of kaolinite-DMSO and kaolinite-N-methylformamide complexes with methanol. The methoxy-functionalized kaolinite organo-complexes were thermally stable, even above 350°C. Fourier transform infrared (FTIR) and nuclear magnetic resonance (NMR) studies revealed that every third inner-surface hydroxyl group was replaced by a methoxy group, keying into the siloxane cavity. Tunney & Detellier (1997) used reagents with amino-functional groups to modify the inner surface chemically. Thus, the Al–$OCH_2CH_2NH_2$ groups keying into the hexagonal cavity of the siloxane layers may contribute to the interactions made by the H-bonds in the interlamellar space.

Starting from kaolinite-DMSO precursors, several kaolinite organo-complexes were synthesized by Gardolinski & Lagaly (2005a) using alkanol, diol and glycol monoether reagents. These reagents form esters with the inner-surface HO groups. Gardolinski & Lagaly (2005b) also exfoliated *n*-alkylamine-kaolinite complexes successfully by washing with toluene followed by ultrasonic treatment resulting in tubular structures. The (hydrophilic/hydrophobic) properties of the nanotubes formed may be controlled by the reagents used. Starting from a kaolinite-DMSO complex, Patakfalvi *et al.* (2004) intercalated silver nanoparticles within the interlamellar space. Dékány *et al*. (2004, 2008) synthesized Ag-, Pd- and Rh-containing kaolinite complexes from a kaolinite-DMSO precursor. Starting from thermally dehydrated kaolinite-potassium acetate (K-KAc), Janek *et al.* (2007) obtained ethylene glycol- and glycerol-containing kaolinite complexes.

Letaief & Detellier (2008, 2009b) studied the possibility of intercalating ionic liquids into kaolinite. During synthesis of quaternary-ammonium salts and reaction with Na-polyacrylate in the interlayer space, rolling-up of kaolinite sheets and formation of nanotubes was observed (Letaief & Detellier, 2009a). Letaief *et al.* (2011) intercalated ionic liquids into kaolinite-DMSO and kaolinite-urea complexes. With the *in situ* polymerization of the ionic liquid, different morphologies were obtained: nanocomposites (exfoliation) with kaolinite-urea precursors, while with kaolinite-DMSO precursors microcomposites (aggregation) were formed.

The present and other authors have carried out extensive studies on the selection of potential precursor complexes and the elucidation of their structures (Makó *et al.*, 2009, 2014; Horváth *et al.*, 2005, 2011; Kristóf *et al.*, 1998, 1999; Frost *et al.*, 1999b, 2000a).

Tracking the results of intercalation and surface modification requires a variety of advanced analytical techniques, especially X-ray diffraction (XRD), vibrational spectroscopy (FTIR, Raman), NMR and thermal analysis (TA). These investigations are often complemented with specific surface area and pore-volume distribution measurements. However, a more complex interpretation of surface reactions at the atomic level often requires the use of molecular modelling and various computational chemical methods (Táborosi *et al.*, 2014a, b).

In spite of the great volume of published work dealing with the preparation and structure elucidation of layer structured minerals (kaolinites, brucite, layered double hydroxides) and metal colloid-containing hybrid materials, there are several open questions due to the differences in their structural and surface properties. In the present work the effects of structural order, the different reaction pathways and the influence of precursor preparation methods on the morphology of the nanostructures obtained via replacement intercalation of kaolins, are discussed in detail. Understanding the morphology and surface properties of nanostructures is vital in light of their possible applications.

Table 1. Chemical and mineralogical composition of the kaolins used in the present study.

Source	Surmin Poland	Zettlitz Czech	Szegilong Hungary
Composition (% w/w):			
SiO_2	52.1	46.23	46.73
Al_2O_3	34.1	36.74	33.94
Fe_2O_3	0.60	0.88	3.21
K_2O	0.6	0.66	0.22
Na_2O	0.1	–	0.1
MgO	0.1	0.28	0.15
CaO	0.1	0.80	0.55
TiO_2	0.60	0.05	0.06
Quartz	12	2	3
Kaolinite/halloysite content	82	91	46/49
Other minerals	5	7	2
Loss on ignition	11.8	13.36	14.12
Specific surface area (m^2/g)	10.3	19.4	31.3
Hinckley index (HI):	1.4	0.8	0.3
Structure	ordered	semi-ordered	disordered

https://doi.org/10.1180/claymin.2015.050.3.06 Published online by Cambridge University Press

EXPERIMENTAL

Materials

For the preparation of the nanostructures three kaolin samples of varying structural order were used. The chemical compositions of the raw kaolins are given in Table 1. The untreated kaolins were ground in an agate mortar and dry-sieved through a 125 μm sieve. The reagents used: potassium acetate (KAc, Reanal), ethylene glycol (EG, Sigma-Aldrich, anhydrous 99.8%), *n*-hexylamine (HA, Sigma-Aldrich), toluene (Reanal), urea (Sigma Aldrich), 2-propanol (IPA, Fluka) , triethanolamine (TEA, Sigma-Aldrich), iodomethane (MeI, Sigma-Aldrich), sodium polyacrylate (PAS, Sigma-Aldrich) and acetone (Ac, Reanal), were of analytical grade.

Synthesis of the nanostructures

The publications of Letaief & Detellier (2009a), Janek *et al.* (2007) and Gardolinsky & Lagaly (2005b) were used in the planning of the reaction pathways. Basically, two different routes were used for the preparation of the nanostructures (Table 2). In Method 1, starting from a kaolinite-urea precursor, the d_{001} spacing was increased to 11.0 Å with TEA. Then, using MeI, a triethylmethylammonium iodide was synthesized in the interlamellar space, further expanding the basal spacing to 11.6 Å. Changing the I^- counter-ions to polyacrylate anions separated the layers, resulting in a nanostructure consisting of disordered TO layers. The efficiency of exfoliation through steps 1 to 4 was at least 93%, calculated from XRD data using the basal peak intensities (Wiewióra & Brindley, 1969).

In Method 2 the kaolinite-KAc precursor was prepared in two different ways. In Method 2.1A the kaolin was mixed with KAc at a 70:30 mass ratio and then exposed to the atmosphere for 3 days. During this period an intercalation efficiency of ~93% was achieved, calculated from XRD data using the basal peak intensities. Subsequently, the complex was washed with IPA and dried overnight at 110°C. In Method 2.1B, kaolin (1 g) was mixed with 8 M KAc solution (100 mL) and stirred at room temperature for

Table 2. Summary of the synthesis routes used.

Method 1 Precursor reagent: urea (U)		Method 2 Precursor reagent: potassium acetate (KAc)	
Reagents	Complex preparation steps	Reagents	Complex preparation steps
U	PRECURSOR (step 1.1) co-grinding Letaief & Detellier (2009a), washing with IPA, drying at 25°C	KAc	PRECURSOR (step 2.1) 2.1A homogenization Makó *et al.* (2014) 2.1B 8 M aqueous solution washing, drying at 110°C for 12 h
TEA	GRAFTING (step 1.2) 1:6 precursor:TEA 180°C, 2 h separation, washing with IPA drying at 60°C for 2 h	EG	REPLACEMENT INTERCALATION (step 2.2A) 1 g precursor + 7 mL EG 150°C, 2 h, Ar atmosphere separation, washing with Ac drying at 70°C for 12 h REPLACEMENT INTERCALATION (step 2.2B) heating with MW, 150°C, 30 min
MeI	QUATERNARIZATION (step 1.3) 1 g complex 2 + 10 mL MeI boiling for 72 h separation, washing with IPA	HA	REPLACEMENT INTERCALATION (step 2.3) 1 g complex 2 + 5 mL HA room temp., 48 h separation, washing with Ac drying at room temp., 12 h drying at 50°C for 2 h
PAS	EXFOLIATION (step 1.4) 1 g complex 3 + 5 g PAS grinding for 1 h at 20°C separation, washing with Ac	T	EXFOLIATION (step 2.4) 1 g complex 3 + 5 mL T room temp., 2 h separation, washing with Ac

https://doi.org/10.1180/claymin.2015.050.3.06 Published online by Cambridge University Press

TABLE 3. Basal distances after the different steps of intercalation. The d(001) values are independent of the HI values of the treated kaolinites.

	Method 1		Method 2	
	Reagent kaolinite	d_{001} Å 7.2	Reagent kaolinite	d_{001} Å 7.2
1	U	10.7	KAc	14.1
2	TEA	11.0	EG	10.8
3	$R'R_3N^+I^-$	11.6	HA	26.5
4	PAS	N/M	T	N/M

80 h. After centrifugation the sample was rinsed with 0.2 μS/cm water and washed with acetone. The exchange-intercalation with EG reagent was done by two different means. In Method 2.2A the kaolinite-KAc was contact heated under an Ar atmosphere with continuous stirring. In Method 2.2B microwave heating was used (Table 2). Then, the EG was replaced by HA, when the basal distance changed from 11.0 Å to 26.5 Å, and complete exfoliation was attained after washing with toluene.

Usually, a single treatment with HA resulted in exfoliation, however, in order to increase the efficiency of the EG→HA replacement intercalation to >93%, step 3 may need to be repeated two to three times. In addition, Gardolinski & Lagaly (2005b) showed that the d_{001} value of the kaolinite-HA organo-complex is influenced by the quality of the reagent used in the previous step; i.e. water-free reagents and an inert atmosphere appear critical to the efficiency of steps 2 and 3.

Structure elucidation methods

X-ray powder diffraction (XRD) analyses were carried out with a Philips PW 3710-type instrument (Cu*K*α radiation, λ = 1.54056 Å, 50 kV, 40 mA), in the 4° to 40°2θ range with a scanning speed of 0.02°/s. The efficiency of the synthesis steps were followed by XRD using back-packed mounts of finely powdered samples to eliminate preferential orientation.

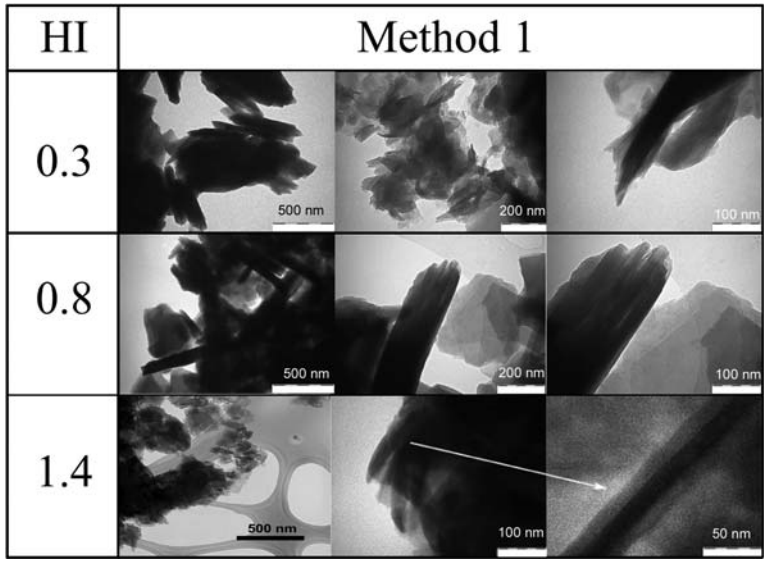

FIG. 1. TEM images of the nanostructures prepared by Method 1 at various magnifications.

https://doi.org/10.1180/claymin.2015.050.3.06 Published online by Cambridge University Press

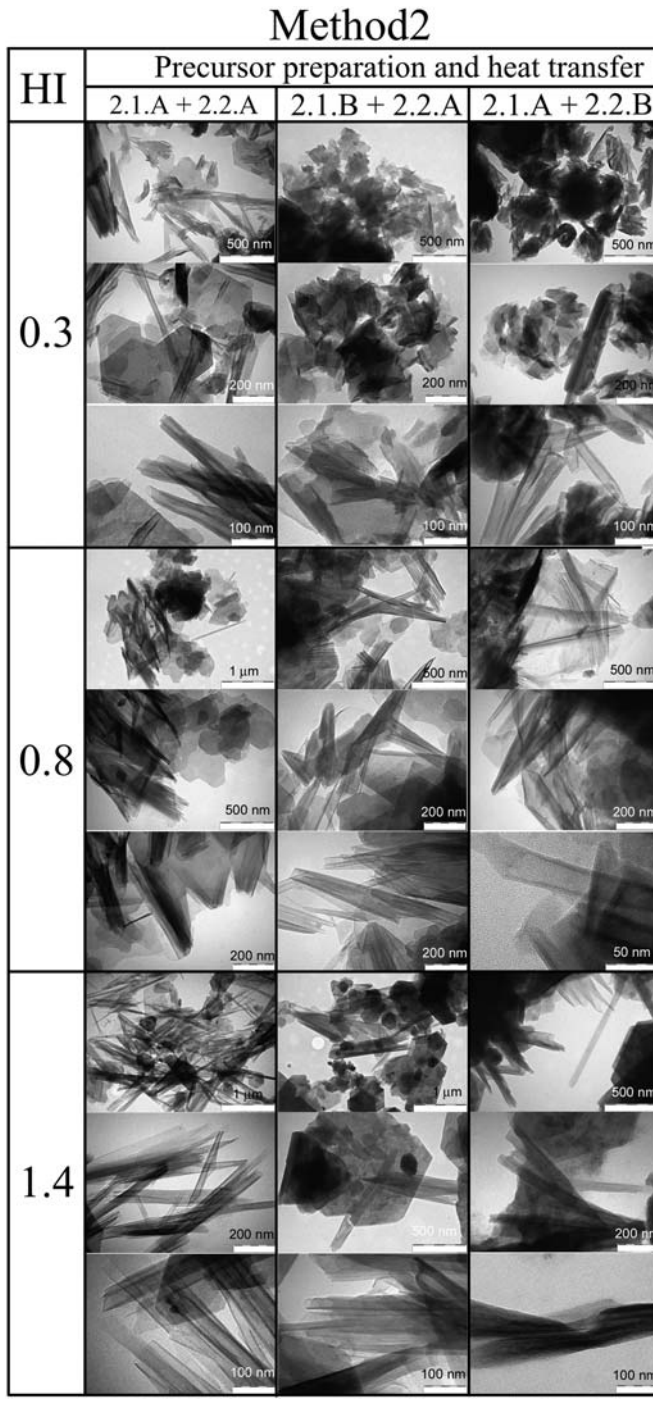

FIG. 2. TEM images of the nanostructures prepared by Method 2. Precursor preparation with homogenization (2.1A); with 8 M KAc solution (2.1B) and replacement intercalation with EG reagent with direct heating (2.2A); with MW heating (2.2B).

https://doi.org/10.1180/claymin.2015.050.3.06 Published online by Cambridge University Press

Fourier-transform infrared (FTIR) spectroscopic measurements were made used a BRUKER Vertex 70 spectrometer with a Bruker Platinum ATR adapter. The spectra were recorded at a resolution of 2 cm^{-1} with a room-temperature DTGS detector (1024 scans were co-added). The spectra were processed with the Thermo Fischer Scientific GRAMS/Al version 9.0 and the Jandel Scientific PeakFit version 4 program for Win32.

Transmission electron microscopy (TEM) images were obtained with a MORGAGNI 268D TEM. The samples were washed with solvents of varying polarity, separated by centrifugation, then suspended in ethanol before placing on a Formvar®-coated copper grid.

Molecular mechanics (MM) calculations were carried out with the Spartan 10 program (Wavefunction Inc., CA, USA), using the MMFF94 parameter set (Halgren, 1996). To build up the TO layers the *American Mineralogist* Crystal Structure database (Viani *et al.*, 2002), as well the FTIR, Raman, XRD and TA experimental data obtained in the present study were used. A monolayer arrangement of the reagents was assumed in the interlayer space and, of the weak interactions, only the H bonds were taken into account.

RESULTS AND EVALUATION

Preparation of kaolinite nanostructures

The basal distances produced at each preparation step are summarized in Table 3. Urea was used instead of the DMSO proposed by Letaief & Detellier (2009a) for the synthesis of the precursor. Since poorly ordered kaolinites (e.g. Szegilong, Hungary, Hinkley-index (HI) = 0.3) can be intercalated only poorly in aqueous suspension, the kaolinite-urea precursors were also prepared, for comparison purposes, by co-grinding the highly ordered kaolinites (Table 2). An intercalation efficiency of ~100% may be achieved easily. Unfortunately, the tetraalkylammonium polyacrylate adsorbs strongly at the kaolinite surface, causing difficulties in interpretation of the TEM and FTIR results.

In Method 2 the preparation of the precursor followed the procedure of Makó *et al.* (2014) and a complete exfoliation was achieved using a 3-step replacement intercalation process. The precursor was made with a physical mixture under an atmosphere of 60% relative humidity. Thus, water plays a definite role in the first step of layer expansion. This is especially important as the sample needs to be heated before the second step of replacement intercalation with EG. Water loss can also be followed with XRD at 200°C as the 14.1 Å spacing collapses partially to *d* spacings of 11.5 and 8.9 Å. Based on the results from high-temperature Raman spectroscopy, it is concluded that the 14.1 Å reflection represents a vertical orientation of the acetate ions in the complex connecting to the inner surface HO groups through water molecules. The 11.5 Å reflection represents the direct connection of the acetate ions to the inner surface HO groups without water. The 8.9 Å reflection is due to the orientation of the acetate ion parallel to the *ab* plane (Frost *et al.*, 2000b,c, 2001, 2003). It should be noted, however, that the crystalline potassium-acetate also has a reflection at 8.9 Å (Kristóf *et al.*, 1997).

In contrast to the kaolinite-DMSO complex, the kaolinite-urea precursor does not react with EG, indicating the complex-stabilizing effect of water. When the reagent is connected to the inner layer surface through a water molecule, stronger H bonds may form, increasing the stability of the complex. When the reagent does not connect to the kaolinite layer through water (e.g. in the DMSO complexes when water molecules form bridges between the reagent molecules), the stability of the complex decreases (Kristóf *et al.*, 1999; Frost *et al.*, 1999a,b, 2000a; Martens *et al.*, 2002). With the use of water-free reagents the strength of the H bonds may be reduced and higher rates of exfoliation may be achieved.

Transmission electron microscopic (TEM) studies

Typical TEM images of the nanostructures obtained by Methods 1 and 2 are given in Figures 1 and 2. Some of the PAS reagent is still adsorbed on the surfaces of the samples prepared by Method 1, despite washing with solvents of varying polarity. This can be an advantage when the nanoparticles are dispersed in a polymer matrix (strengthening the interaction between the particles and the matrix) (Khunova *et al.*, 2013).

A reduction in particle size can be observed, irrespective of the structural order, for both the tubular/halloysite-like and the pseudo-hexagonal/chip-like structures. The length of the tubes, obviously reduced by dry grinding, is 100–200 nm. As the particles become aggregated, it is difficult to determine the real diameter of the nanotubes. However, they are definitely larger than the theoretical value of 24–25 Å.

https://doi.org/10.1180/claymin.2015.050.3.06 Published online by Cambridge University Press

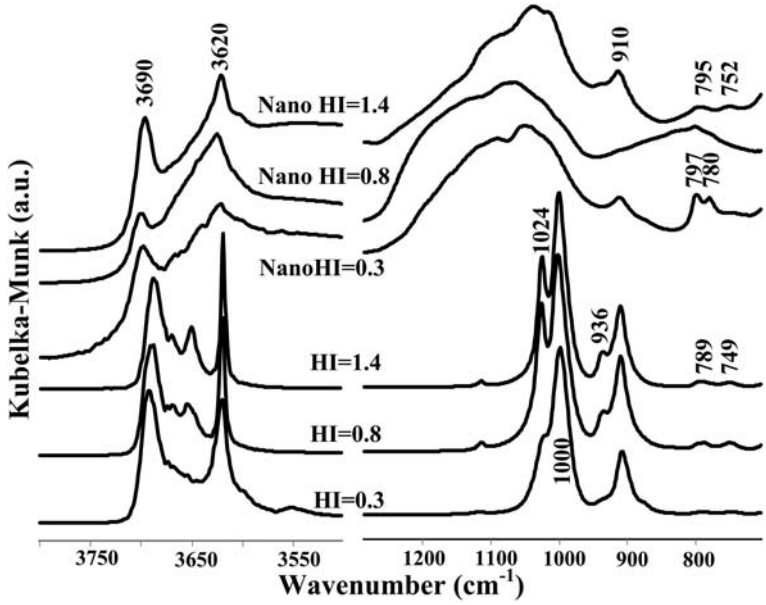

FIG. 3. FTIR spectra of kaolins of variable structural order and their nanostructures in the OH and Si-O spectral ranges (Method 1).

The predominant form of the nanostructures formed during the 3-step replacement intercalation process is tubular (Method 2). The replacement-intercalation and the exfoliation of the precursor complex formed from the mechanical mixture under a humid atmosphere results in a tubular morphology of a few hundred

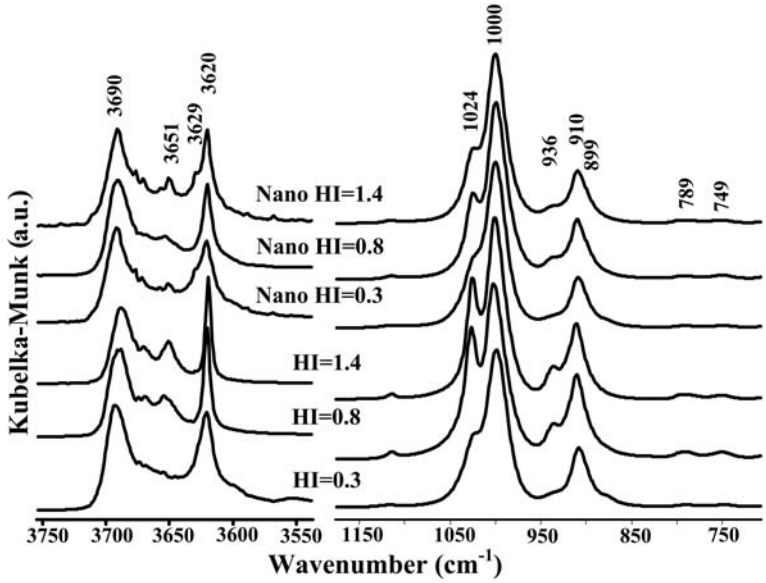

FIG. 4. FTIR spectra of kaolins with variable structural order and their nanostructures in the OH and Si–O spectral ranges (Method 2).

https://doi.org/10.1180/claymin.2015.050.3.06 Published online by Cambridge University Press

nanometers, or occasionally a few μm, in length with a typical diameter between 25–30 nm. The proportion of the particles with hexagonal- or chip-like morphology reduces with an increase in the structural order (Fig. 2, column 1, Figures 2.1A + 2.2A). The hexagonal structures dominate when either mechanical (Method 2.1B) or microwave means (Method 2.2B) are used during the preparation of the precursor (Fig. 2).

Characterization of the nanostructure with FTIR spectroscopy

A comparison of the FTIR spectra of the nanostructures obtained by the two different methods, with those of the untreated kaolinites, are shown in Figures 3 and 4 and the assignments of the IR bands are summarized in Table 4. The FTIR spectra of the nanostructures produced by Method 1 show a mixture of the bands of the PAS used for the exfoliation and those of the nanoparticles formed, in agreement with the results presented in previous sections. In spite of the difficulties caused by the matrix effects of the PAS, the ratios of the H–O stretching bands can be related to the morphology, rather than simply to the structural order. The deformation band of the inner OH groups is broader than in the untreated mineral as a result of changes in orientation caused by the changing chemical environment.

An interesting feature of the nanostructure is the shift of the 3690 cm^{-1} HO band by 5 cm^{-1} to higher frequencies. If the nanostructures are either open tubes with larger diameters, or quasi-hexagonal platelets, it is logical to suppose that the observed shift results from the decreasing interaction between the surface OH groups and the reduced adsorption of water. The tetraalkylammonium polyacrylate reagent causes spectral interference and significant band broadening in the Si–O stretching and OH deformation ranges.

The FTIR spectra of the nanostructures obtained by the 3-step replacement intercalation method (Method 2) shows no matrix effects as the surface can be cleaned with Ac and IPA and the residual solvent can be removed by gentle heating. In the FTIR spectra of the nanostructures, the 3690/3620 cm^{-1} and the 1024/1000 cm^{-1} band ratios differ significantly from those in the original mineral (Fig. 4). In addition, the 910 cm^{-1} band becomes broader, while a strongly overlapping band occurs at 899 cm^{-1}. Since the clean kaolinite nano-surfaces can adsorb significant amounts of water from the atmosphere, the changes in spectra can be due to an altered secondary structure/morphology and to a modified chemical environment caused by water adsorption. Janek *et al.* (2007) observed that in the kaolinite-KAc complex, the chemical environment might modify the orientation of the inner OH groups. Táborosi *et al.* (2014a, b) showed with HF and DFT calculations that the adsorbed solvents can change the orientation of the surface OH groups in the exfoliated TO layers, thereby influencing the donor-acceptor properties and the orientation of the inner surface OH groups as well. In the periodic model they built up from experimental data, the change in orientation resulted in changes in the HO–Al, Al–apical O and apical O–Si bond lengths.

The TO layer cannot be considered as a "compact" structure, thus, changes in the interactions of the surface HO groups can result in changes in both the bond lengths and angles and the establishment of new equilibrium bond strengths. These new equilibria are represented by changes in the ratios and broadening bands for the Si–O and H–O valence and deformation vibrations. Thus, the inner HO groups are sensitive to the changes in the chemical environment.

Table 4. Assignment of FTIR bands for untreated and exfoliated kaolinites.

Wavenumber (cm^{-1})	Attribution of bands
3690–3629	OH stretching of inner-surface hydroxyl, untreated kaolinite OH stretching of surface hydroxyl, kaolinite nanostructure
3620	OH stretching of inner hydroxyl (AlAlOH)
1024–1000	Si–O stretching (in-plane)
936	OH deformation of inner-surface hydroxyl, untreated kaolinite OH deformation of surface hydroxyl, kaolinite nanostructure
910	OH deformation of inner hydroxyl (AlAlOH)
899	OH deformation of surface hydroxyl (bonded), kaolinite nanostructure
790; 749	Si–O bending

Molecular mechanics calculations

With the use of suitable force fields, molecular mechanics models can describe the structure of the high atom number systems precisely, but they give less

https://doi.org/10.1180/claymin.2015.050.3.06 Published online by Cambridge University Press

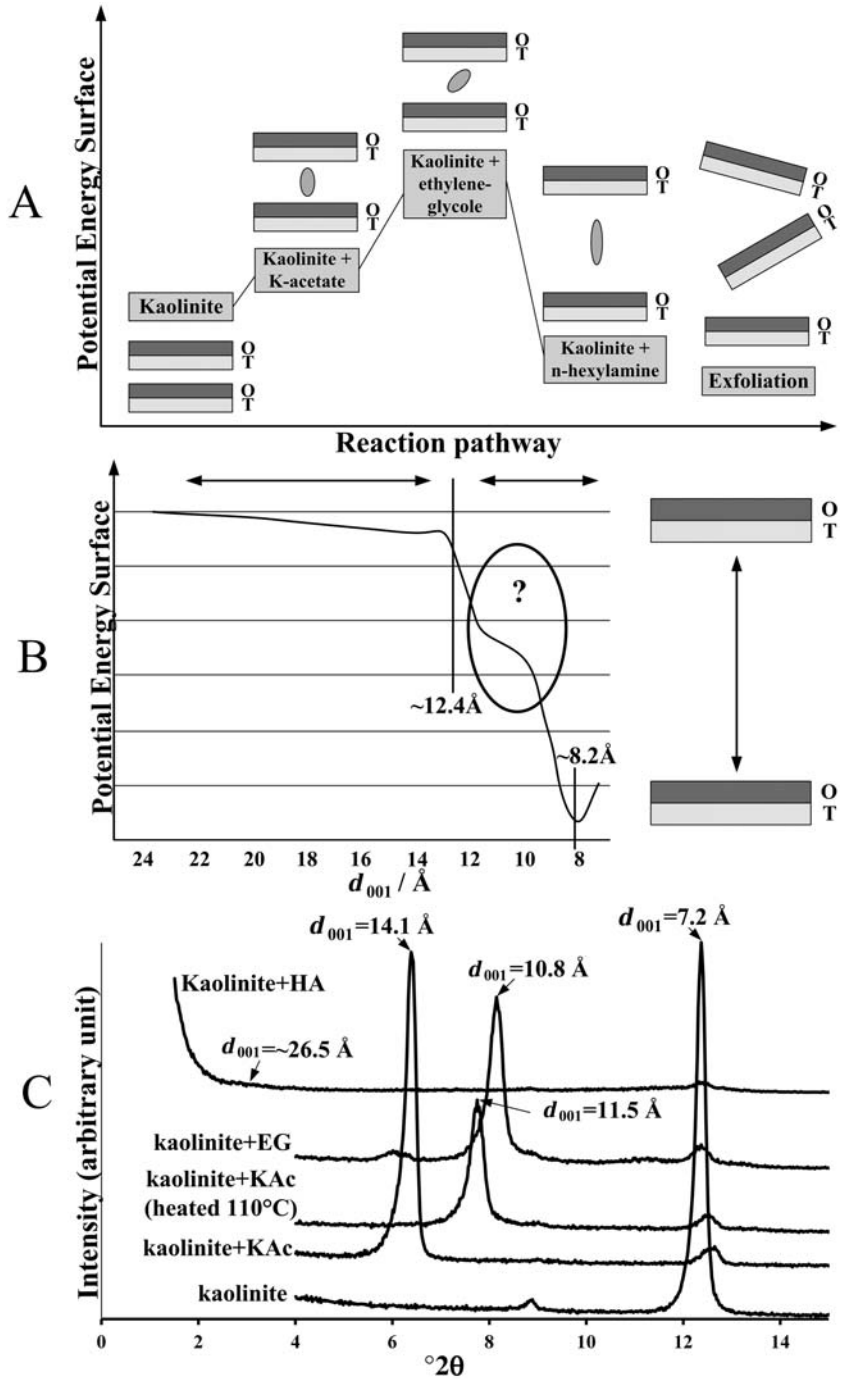

FIGURE 5. (A) Schematic representation of the system energies obtained by the MMFF94 parameter set; (B) change of the potential energy surface (PES) as a function of the d_{001} basal distance; (C) representative XRD curves and the corresponding d_{001} values of the organo-complexes prepared by Method 2. Due to exfoliation the 26.5 Å reflection is missing (see more in the 'Synthesis of the nanostructures' section).

https://doi.org/10.1180/claymin.2015.050.3.06 Published online by Cambridge University Press

accurate results for potential energy surfaces (PES) (Cramer, 2004). For low atom number systems, accurate results can be obtained with the density functional theory (DFT) method. However, for systems with large numbers of atoms, the calculation of potential energy surfaces with the DFT method is lengthy, even with high-capacity computers. Although the computational time for the molecular mechanics model is shorter, the results obtained are often erroneous. However, if, during the calculations, parameters like the number of atoms or the types of interactions are kept constant, the resultant energy values (in spite of their inherent inaccuracy) can be used to set up a relative sequence, which can be useful for planning experiments or interpreting experimental results. Figure 5 shows the relative potential energy surfaces of the organo-complexes prepared by Method 2. Up to the step of preparing the kaolinite-EG complex the process needs an input of energy, while the exchange intercalation with HA and the exfoliation with toluene results in energy release. Because the d_{001} spacing in kaolinite-HA complex is much greater than the size of the reagent, a multi-layer is probably formed in the interlamellar space allowing TO/HA–HA/TO interactions, also.

Figure 5B shows the calculated potential energy surface values as a function of the basal distance. The function has a minimum at 8.2 Å for kaolinite, which is 1 Å greater than the experimental layer distance of 7.2 Å. In order to decrease this discrepancy a modified parameter set will be used. As the basal distance increases, an inflection point occurs at 10–11 Å (Fig. 5B). This appears to be a critical value above which exfoliation can be attempted, if the stabilizing effect of water is taken into consideration. Practically no interaction exists between the TO layers with basal distances >12–13 Å. Considering the basal distance of the water-free kaolinite-EG complex (10.8 Å) (Fig. 5C), as well as the fact that with Method 2 ~93% exfoliation can be achieved with hexylamine during the third step of the exchange intercalation reaction, the molecular mechanics model can be used to describe the process of exfoliation reasonably well.

CONCLUSIONS

Kaolinite nanostructures were prepared by two different methods from three kaolins with varying degrees of structural order (high, intermediate and low). Method 1 produced pseudo-hexagonal and tubular-type nanostructures, but the lengths of the tubes were rather short, due to the precursors being formed by mechanochemical treatment (dry grinding). Method 2, a 3-step intercalation process, produced tubular, or halloysite-like nanostructures mainly, with smaller amounts of pseudo-hexagonal or chip-like particles. With kaolinites of greater structural order, the tubular morphology dominates. The length of the tubes was influenced by the method of preparation of the precursor and by the type of heat treatment during the 2nd process step (i.e. preparation of the kaolinite-EG complex). The preparation of the precursor, from either an 8 M aqueous KAc solution or by microwave treatment, resulted in cracked, broken tubes and appeared to increase the formation of chip-like particles. The efficiency of each preparation depended on the water content of the intercalation reagents and on the hydration quality of the atmosphere used. The reagent used in the final step, along with the extracting solvent toluene, were removed efficiently from the surface. The nanostructures obtained may have potential use for the production of nano-hybrids and catalysts/catalyst supports.

In the FTIR investigations, the ratios of the bands due to the surface and inner HO groups and to the Si–O stretching vibrations, differ significantly from those of the untreated kaolinite. In addition, the deformation band of the inner HO group, at 910 cm^{-1}, displayed significant broadening. In the nanostructures, changing the positions of the surface HO groups usually resulted in altered orientations of the inner HO groups, producing a changing dipole moment and leading to a change in the FTIR band intensity and broadening. The changing coordinates of the inner-surface HO groups influences the HO–Al, apical O–Al and apical O–Si bond lengths, thus modifying the band ratios, proving that the inner HO group is not an inert group. Molecular mechanics calculations confirmed that the kaolinite organo-complexes could be exfoliated efficiently with water-free, weak H-bonding reagents within the interlayer space to produce hybrid kaolinite materials with 10–13 Å basal spacing.

ACKNOWLEDGEMENTS

The authors gratefully acknowledge the financial support of the European Union and the European Social Fund via the framework project TÁMOP-4.2.2.A-11/1/KONV-2012-0071. The authors thank both Prof. R. K. Szilágyi for his help in the interpretation of the computational chemical results and Dr J. Matusik for providing the Surmin kaolin.

REFERENCES

Araújo F.R., Baptista J.G., Marcal L., Ciuffia K.J., Nassara E.J., Calefi P.S., Vicente M.A., Trujillano R., Rives V., Gilc A., Korilic S. & de Fariaa E.H. (2014) Versatile heterogeneous dipicolinate complexes grafted into kaolinite: Catalytic oxidation of hydrocarbons and degradation of dyes. *Catalysis Today*, **227**, 105–115.

Brigatti M.F., Galán E. & Theng B.K.G. (2006). Structures and mineralogy of clay minerals. Pp. 19–24 and 26–30 in: *Handbook of Clay Science. Advances in Clay Science*, 1st edition (Bergaya F., Theng B.K.G. & Lagaly G., editors). Elsevier, Amsterdam.

Bizaia N., De Faria E.H., Ricci G.P., Calefi P.S., Nassar E. J., Castro K.A.D.F., Nakagaki S., Ciuffi K.J., Trujillano R., Vicente M.A., Gil A. & Korili S.A. (2009) Porphyrin-kaolinite as efficient catalyst for oxidation reactions. *ACS Applied Materials and Interfaces*, **1**, 2667–2678.

Cramer J.C. (2004) *Essentials of Computational Chemistry, Theories and Models*, 2nd edition, pp. 6–10, John Wiley & Sons Ltd., Chichester, UK.

De Faria, E.H., Ricci G.P., Marçal L., Nassar E.J., Vicente M.A., Trujillano R., Gil A., Korili S.A., Ciuffi K.J. & Calefi P.S. (2012) Green and selective oxidation reactions catalyzed by kaolinite covalently grafted with Fe(III) pyridine-carboxylate complexes. *Catalysis Today*, **187**, 135–149.

Dedzo G.K. & Detellier C. (2014) Intercalation of two phenolic acids in an ionic liquid-kaolinite nanohybrid material and desorption studies. *Applied Clay Science*, **97–98**, 153–159.

Frost R.L., Kristóf J., Horváth E. & Kloprogge J.T. (1999a) Deintercalation of dimethylsulphoxide intercalated kaolinites – a DTA/TGA and Raman spectroscopic study. *Thermochimica Acta*, **327**, 155–166.

Frost R.L., Kristóf J., Horváth E. & Kloprogge J.T. (1999b) Molecular structure of dimethyl sulphoxide in DMSO-intercalated kaolinites at 298 and 77 K. *Journal of Physical Chemistry A*, **103**, 9654–9660.

Frost R.L., Kristóf J., Horváth E. & Kloprogge J.T. (2000a) Kaolinite hydroxyls in dimethylsulphoxide intercalated kaolinites at 77K – a Raman spectroscopic study. *Clay Minerals*, **35**, 443–454.

Frost R.L., Kristóf J., Horváth E. & Kloprogge J.T. (2000b) Rehydration and phase changes of potassium acetate-intercalated halloysite at 298 K. *Journal of Colloid and Interface Science*, **226**, 318–327.

Frost R.L., Kristóf J., Horváth E. & Kloprogge J.T. (2001) Raman spectroscopy of potassium acetate-intercalated kaolinites over the temperature range 25 to 300°C. *Journal of Raman Spectroscopy*, **32**, 271–277.

Frost R.L., Kristóf J., Kloprogge J.T. & Horváth E. (2000c) Rehydration of potassium acetate-intercalated kaolinite at 298 K. *Langmuir*, **16**, 5402–5408.

Frost R.L., Kristóf J., Makó É & Horváth E. (2003) A DRIFT spectroscopic study of potassium acetate intercalated mechanochemically activated kaolinite. *Spectrochimica Acta – Part A: Molecular and Biomolecular Spectroscopy*, **59**, 1183–1194.

Gardolinski J.E.F.C. & Lagaly G. (2005a) Grafted organic derivatives of kaolinite: I. Synthesis, chemical and rheological characterization. *Clay Minerals*, **40**, 537–546.

Gardolinski J.E.F.C. & Lagaly G. (2005b) Grafted organic derivatives of kaolinite: II. Intercalation of primary n-alkylamines and delamination. *Clay Minerals*, **40**, 547–556.

Halgren T.A. (1996) Merck molecular force field. I. Basis, form, scope, parameterization, and performance of MMFF94. *Journal of Computational Chemistry*, **17**, 490–641.

Horváth E., Kristóf J., Kurdi R., Makó É. & Khunová V. (2011) Study of urea intercalation into halloysite by thermoanalytical and spectroscopic techniques. *Journal of Thermal Analysis and Calorimetry*, **105**, 53–59.

Horváth E., Kristóf J., Frost R.L., Jakab E., Makó E. & Vágvölgyi, V. (2005) Identification of superactive centers in thermally treated formamide-intercalated kaolinite. *Journal of Colloid and Interface Science*, **289**, 132–138.

Janek M., Emmerich K., Heissler S. & Nüesch R. (2007) Thermally induced grafting reactions of ethylene glycol and glycerol intercalates of kaolinite. *Chemistry of Materials*, **19**, 684–693.

Khunova V., Kristóf J., Kelnar L. & Dybal J. (2013) The effect of halloysite modification combined with in situ matrix modifications on the structure and properties of polypropylene/halloysite nanocomposites. *eXPRESS Polymer Letters*, **7**, 471–479.

Kristóf J., Frost R.L., Kloprogge J.T., Horváth E. & Gábor M. (1999) Thermal behaviour of kaolinite intercalated with formamide, dimethylsulphoxide and hydrazine. *Journal of Thermal Analysis and Calorimetry*, **56**, 885–891.

Kristóf J., Frost R.L., Horvath E., Kocsis L. & Inczedy J. (1998) Thermoanalytical investigations on intercalated kaolinites. *Journal of Thermal Analysis*, **53**, 467–475.

Kristóf J., Tóth M., Gábor M., Szabó P. & Frost R.L. (1997) Study of the structure and thermal behaviour of intercalated kaolinites. *Journal of Thermal Analysis*, **49**, 1441–1448.

Letaief S. & Detellier C. (2008) Ionic liquids-kaolinite nanostructured materials. Intercalation of pyrrolidinium salts. *Clays and Clay Minerals*, **56**, 82–89.

Letaief S. & Detellier C. (2009a) Clay-polymer nanocomposite material from the delamination of kaolinite in the presence of sodium polyacrylate. *Langmuir*, **25**, 10975–10979.

Letaief S. & Detellier C. (2009b) Functionalization of the interlayer surfaces of kaolinite by alkylammonium

https://doi.org/10.1180/claymin.2015.050.3.06 Published online by Cambridge University Press

groups from ionic liquids. *Clays and Clay Minerals*, **57**, 638–648.

Letaief S., Leclercq J., Liu Y. & Detellier C. (2011) Single kaolinite nanometer layers prepared by an in situ polymerization-exfoliation process in the presence of ionic liquids. *Langmuir*, **27**, 15248–15254.

Makó E., Kristóf J., Horváth E., Vágvölgyi, V. (2009) Kaolinite-urea complexes obtained by mechanochemical and aqueous suspension techniques – A comparative study. *Journal of Colloid and Interface Science*, **330**, 367–373.

Makó É., Kovács A., Horváth E. & Kristóf J. (2014) Kaolinite-potassium acetate and halloysite-potassium acetate complexes prepared by mechanochemical, solution and homogenization techniques: A comparative study. *Clay Minerals*, **49**, 457–471.

Martens W.N., Frost R.L., Kristóf J. & Horváth E. (2002) Modification of kaolinite surfaces through intercalation with deuterated dimethyl sulphoxide. *Journal of Physical Chemistry B*, **106**, 4162–4171.

Matusik J. & Bajda T. (2013) Immobilization and reduction of hexavalent chromium in the interlayer space of positively charged kaolinites. *Journal of Colloid and Interface Science*, **398**, 74–81.

Matusik J. & Matykowska L. (2014) Behaviour of kaolinite intercalation compounds with selected ammonium salts in aqueous chromate and arsenate solutions. *Journal of Molecular Structure*, **1071**, 52–59.

Matusik J., Stodolak E. & Bahranowski, K. (2011) Synthesis of polylactide/clay composites using structurally different kaolinites and kaolinite nanotubes. *Applied Clay Science*, **51**, 102–109.

Nakagaki S., Machado G.S., Halma M., dos Santos Marangon A.A., de Freitas Castro K.A.D., Mattoso N. & Wypych F. (2006) Immobilization of iron porphyrins in tubular kaolinite obtained by an intercalation/delamination procedure. *Journal of Catalysis*, **242**, 110–117.

Papp S., Patakfalvi R. & Dékány I. (2008) Metal nanoparticle formation on layer silicate lamellae. *Colloid and Polymer Science*, **286**, 3–14.

Papp S., Patakfalvi R. & Dékány I. (2004) Synthesis and characterization of noble metal nanoparticles/kaolinite composites. *Progress in Colloid and Polymer Science*, **125**, 88–95.

Patakfalvi R. & Dékány I. (2004) Synthesis and intercalation of silver nanoparticles in kaolinite/DMSO complexes. *Applied Clay Science*, **25**, 149–159.

Rehim M.H.A., Youssef A.M. & Essawy H.A. (2010) Hybridization of kaolinite by consecutive intercalation: Preparation and characterization of hyperbranched poly(amidoamine)–kaolinite nanocomposites. *Materials Chemistry and Physics*, **119**, 546–552.

Táborosi A., Kurdi R. & Szilágyi R.K. (2014a) Adsorption and intercalation of small molecules on kaolinite from molecular modelling studies. *Hungarian Journal of Industry and Chemistry Veszprém*, **42**, 19–23.

Táborosi A., Kurdi R. & Szilágyi R.K. (2014b) The positions of inner hydroxide groups and aluminium ions in exfoliated kaolinite as indicators for external chemical environment. *Physical Chemistry Chemical Physics*, **16**, 25830–25839

Tao Q., Su L., Frost R.L., He H. & Theng B.K.G. (2014) Effect of functionalized kaolinite on the curing kinetics of cycloaliphatic epoxy/anhydride system. *Applied Clay Science*, **95**, 317–322.

Tonlé I.K., Letaief S., Ngameni E., Walcarius A. & Detellier C. (2011) Square wave voltammetric determination of lead(II) ions using a carbon paste electrode modified by a thiol-functionalized kaolinite. *Electroanalysis*, **23**, 245–252.

Tunney J.J. & Detellier C. (1994) Preparation and characterization of two distinct ethylene glycol derivatives of kaolinite. *Clays and Clay Minerals*, **42**, 552–560.

Tunney J.J. & Detellier C. (1996) Aluminosilicate nanocomposite materials. Poly(ethylene glycol)-kaolinite intercalates. *Chemistry of Materials*, **8**, 927–935.

Tunney J.J. & Detellier C. (1997) Interlamellar amino functionalization of kaolinite. *Canadian Journal of Chemistry*, **75**, 1766–1772.

Tunney J.J. (1996) Chemically modified kaolinite. Grafting of methoxy groups on the interlamellar aluminol surface of kaolinite. *Journal of Materials Chemistry*, **6**, 1679–1685.

Viani A., Gualtieri A. & Artioli G. (2002) The nature of disorder in montmorillonite by simulation of X-ray powder patterns. *American Mineralogist*, **87**, 966–975.

Wiewióra A. & Brindley G.W. (1969) Potassium acetate intercalation in kaolinites and its removal: effect of material characteristics. Pp: 723–733 in *Proceedings of the International Clay Conference Tokyo* (L. Heller, editor). Israel University Press, Jerusalem.